Inorganic Chemistry

Article

pubs.acs.org/IC

Environmentally Friendly, One-Pot Synthesis of Ag Nanoparticle-Decorated Reduced Graphene Oxide Composites and Their Application to Photocurrent Generation

Jingqi Tian,[†,‡] Sen Liu,[†] Yingwei Zhang,[†] Haiyan Li,[†] Lei Wang,[†] Yonglan Luo,[†] Abdullah M. Asiri,[§,∥] Abdulrahman O. Al-Youbi,[§,∥] and Xuping Sun*[,†,§,∥]

[†]State Key Lab of Electroanalytical Chemistry, Changchun Institute of Applied Chemistry, Chinese Academy of Sciences, Changchun 130022, Jilin, China

[‡]Graduate School of the Chinese Academy of Sciences, Beijing 100039, China

[§]Chemistry Department, Faculty of Science, King Abdulaziz University, Jeddah 21589, Saudi Arabia

[∥]Center of Excellence for Advanced Materials Research, King Abdulaziz University, Jeddah 21589, Saudi Arabia

Supporting Information

ABSTRACT: In this paper, we develop an environmentally friendly, one-pot strategy toward rapid preparation of Ag nanoparticle-decorated reducd graphene oxide (AgNPs/rGO) composites by heating the mixture of GO and $AgNO_3$ aqueous solution in the presence of sodium hydroxide at 80 °C under stirring. The reaction was accomplished within a short period of 10 min without extra reducing agent. As-synthesized AgNPs/rGO composites have been successfully applied in photocurrent generation in the visible spectral region.

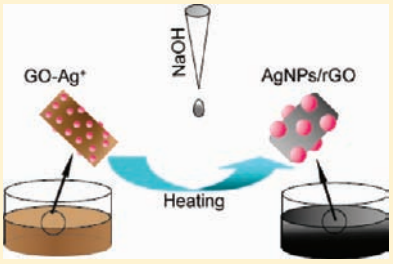

INTRODUCTION

Graphene, a flat monolayer of sp^2-bonded carbon atoms tightly packed into a two-dimensional (2D) honeycomb lattice, has attracted tremendous attention due to its high surface area (~2600 m^2/g), high chemical stability, and unique electronic and mechanical properties.[1] Among the various exciting characteristics, the superior electrical conductivity and mechanical properties make graphene an excellent material for collecting and transporting charge in photoelectrochemical solar cells and photocatalysis.[2] Recently, considerable research efforts have been put into preparing graphene-based composites to increase the efficiency of photocatalysis[3] and solar cells,[4] in which the flat carbon serves as a scaffold to anchor metal or semiconductor nanoparticles and assists in promoting selectivity and efficiency of the catalytic process.[5]

On the other hand, the surface plasmon resonance (SPR) effect of Ag nanoparticles (AgNPs) has recently attracted extensive interest since Awazu et al. proposed the concept of plasmonic photocatalysis.[6] SPR of AgNPs usually results in strong and broad absorption bands in the visible light region, and thus it is exploited to develop visible-light-activated photocatalysts.[7] Inspired by enhancement of the properties of nanoparticles through anchoring them onto reduced graqphene oxide (rGO), researchers have attempted to prepare AgNP-decorated rGO (AgNPs/rGO). Until now, a large number of methods for the synthesis of AgNPs/rGO have been developed successfully.[8] However, the AgNPs/rGOs are usually obtained from in situ reduction of silver salts on the preformed rGO or the decoration of rGO with presynthesized AgNPs, which involve multiple steps and require complex manipulation.[8a−g] Since Hassan et al. reported the microwave-assisted, one-pot preparative method of AgNPs/rGO with the use of oleylamine as the reducing agent,[8h] much attention has been paid to one-pot synthesis of AgNPs/rGO.[8i−n] Unfortunately, the developed methods suffer from the use of hazardous or toxic reducing agents such as $NaBH_4$ and formaldehyde to reduce both GO and Ag^+, posing environmental and health risks, or the involvement of a surface modifier such as poly(*N*-vinyl-2-pyrrolidone) (PVP).

In this paper, we demonstrate an environmentally friendly, one-pot strategy toward rapid preparation of AgNPs/rGO. The formation of AgNPs/rGO is accomplished by directly heating the mixture of GO and $AgNO_3$ aqueous solution in the presence of sodium hydroxide at 80 °C for 10 min under stirring without the extra introduction of other reducing agents and a surface modifier. The central idea used in this approach is that GO serves as a reducing agent for the formation of AgNPs while GO can be converted into rGO at the same time under alkaline conditions. We further demonstrate the successful application of such composites in photocurrent generation in the visible spectral region of white light.

EXPERIMENTAL SECTION

Graphite powder, H_2SO_4, $NaNO_3$, NaOH, $AgNO_3$, and H_2O_2 (30%) were purchased from Aladin Ltd. (Shanghai, China). Ammonia (25 wt

Received: December 30, 2011
Published: March 23, 2012

   dx.doi.org/10.1021/ic300332x | Inorg. Chem. 2012, 51, 4742−4746

%), HCl (36 wt %), and $KMnO_4$ were purchased from Beijing Chemical Corp. The water used throughout all experiments was purified through a Millipore system. GO was prepared from natural graphite powder through a modified Hummer's method[9] using graphite powder, H_2SO_4, $NaNO_3$, and H_2O_2 (30%) as the starting materials. As-synthesized GO was dispersed into individual sheets in distilled water at a concentration of 0.5 mg/mL with the aid of ultrasound for further use. The preparation of AgNPs/rGO was carried out as follows (sample 1): In a typical experiment, 2.2 mL of 8 M NaOH aqueous solution was added dropwise into 20 mL of aqueous dispersion of GO (0.5 mg/mL) containing 2.6 mM $AgNO_3$ at 80 °C under stirring. The solution was washed with water by centrifugation twice, and the resulting precipitate was then redispersed in 20 mL of water and stored at 4 °C for characterization and further use.

UV−vis spectra were obtained on a UV-1800 spectrophotometer. Transmission electron microscopy (TEM) measurements were made on a HITACHI H-8100 electron microscope (Hitachi, Tokyo, Japan) with an accelerating voltage of 200 kV. The sample for TEM characterization was prepared by placing a drop of sample solution on a carbon-coated copper grid and dried at room temperature. Powder X-ray diffraction (XRD) data were recorded on a RigakuD/MAX 2550 diffractometer with Cu Kα radiation (λ = 1.5418 Å). X-ray photoelectron spectroscopy (XPS) analysis was measured on an ESCALABMK II X-ray photoelectron spectrometer using Mg as the exciting source. Raman spectra were obtained on a J-Y T64000 Raman Spectrometer with 514.5 nm wavelength incident laser light. Photoelectrochemical measurements were composed of a CHI 660D electrochemical analyzer (CH Instruments, Inc., Shanghai); a 500 W xenon lamp (CHFXQ500W, Beijing) with an UV cutoff filter (λ > 400 nm, input power: 100 mW/cm^2); and a homemade three-electrode cell using a KCl-saturated Ag/AgCl electrode, a platinum wire, and AgNPs/rGO as the reference, counter, and working electrodes, respectively. The AgNPs/rGO modified indium−tin oxide (ITO) electrode was prepared according to dip-coating method: typically, 100 μL of AgNPs/rGO suspensions was dip-coated onto a 0.5 cm ×4 cm ITO glass electrode. The electrode was then air-dried at room temperature. The supporting electrolyte was 1 M Na_2SO_4, which was purged with high-purity nitrogen for at least 15 min prior to experiments.

RESULTS AND DISCUSSION

Figure 1 shows the Raman spectra of GO and the products thus formed. It is reported that rGO obtained by chemical reduction of GO exhibits two characteristic main peaks: the D band at ~1350 cm^{-1}, arising from a breathing mode of κ-point photons of A_{1g} symmetry, and the G band at 1575 cm^{-1}, corresponding to the first order scattering of the E_{2g} phonon of sp^2 C atoms.[10] In our study, it is seen that both GO and the products exhibit a D band at 1355 cm^{-1} and a G band at 1596 cm^{-1}. The products are also found to show a relatively higher intensity of D to G bands (0.93) than that of GO (0.75). These observations confirm the formation of new graphitic domains after the reaction.[11] Figure 1, inset, shows the photographs of aqueous dispersion of GO (left) and the products thus obtained (right), exhibiting a distinct color change from pale-yellow to black after reaction. Such an observation provides another piece of evidence for the formation of rGO.

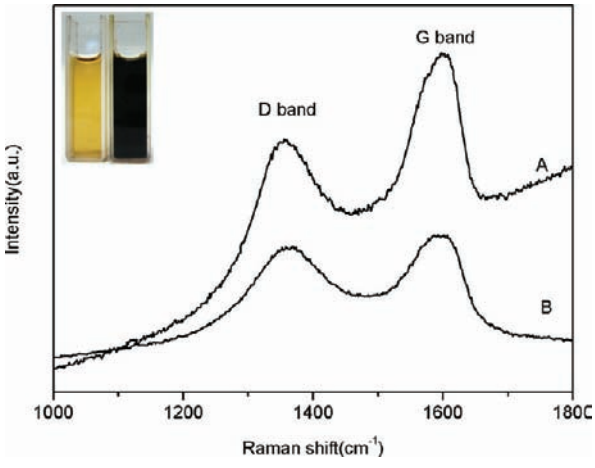

Figure 1. Raman spectra of GO (A) and products thus obtained (B). Inset: photographs of GO (left) and products (right) in aqueous solution.

It is known that most of the oxygen-containing functional groups in GO exist in the form of either hydroxyl or epoxide groups,[12] and the successful removal of epoxy and hydroxyl means the formation of rGO, which can be confirmed by X-ray photoelectron spectroscopy (XPS). Figure 2A and B show the C 1s XPS spectra of GO and the products, respectively. The C 1s spectra of GO and the products could be deconvoluted into four peaks at 284.6, 285.7, 286.7, and 288.2 eV, which are associated with C−C, C−OH, C(epoxy/alkoxy), and C═O, respectively.[13] It is obviously seen that the peak intensity of C−O and C(epoxy/alkoxy) in rGO tremendously decrease, and the content of C−C correspondingly increases dramatically. All of the observations suggest that the most oxygen-containing functional groups are successfully removed after the reaction. It was reported that metallic Ag 3d peaks are centered at 373.9 and 367.9 eV,[14] and the Ag(I) exhibits two peaks at 375.8 and 369.6 eV.[15] However, the Ag 3d peaks in our present study appear at 374.3 and 368.3 eV (Figure 2C), which suggests that there is both metallic Ag and Ag^+ adsorbed in the rGO sheets.

The XRD pattern of the products thus obtained is shown in Figure 3. The four peaks located at 38.0, 44.4, 64.4, and 77.3° are assigned to 111, 200, 220, and 311 faces of a Ag crystal, respectively, demonstrating the formation of metallic Ag.[15] The broad peak at 2θ = 20−30° appears, indicating the disordered stacking of rGO sheets in the composites.[16] On the basis of the results of XPS and XRD characterizations, it indicates that AgNPs and rGO were successfully prepared by heating GO and $AgNO_3$ solution in the presence of NaOH.

Figure 4 shows typical TEM images of the products. After the reaction, a large amount of nanoparticles with diameters of a few nanometers to several tens of nanometers are observed uniformly on the surface of the rGO, as shown in Figure 4A. The arrow clearly shows the edge of the rGO sheet. The high magnification TEM image (Figure 4B) further reveals that the nanoparticles are spherical in shape. The high-resolution transmission electron microscopy (HRTEM) image taken from a typical nanoparticle (Figure 4B, inset) shows clear lattice fringes with an interplane distance measured to be 0.235 nm, corresponding to the (111) plane of Ag crystals.[17] It indicates that these nanoparticles are AgNPs and supports the formation of AgNPs/rGO. It is of importance to note that the AgNPs are anchored on the surface of rGO with a high density.

We also examined the influence of the relative amount of Ag^+ on the AgNPs/rGO composites' formation. Figure 5 shows the corresponding TEM images. When the amount of Ag^+ was increased up to 4-fold (sample 2), a large amount of nanoparticles with diameters ranging from 15 to 30 nm were formed as the main products, as shown in Figure 5A. When the amount of Ag^+ decreases to one-fourth of that used in sample 1 (sample 3), nanoparticles with diameters ranging from a few nanometers to 20 nm were formed as the main products, and the particle density on the rGO sheets decreased tremendously,

dx.doi.org/10.1021/ic300332x | Inorg. Chem. 2012, 51, 4742−4746

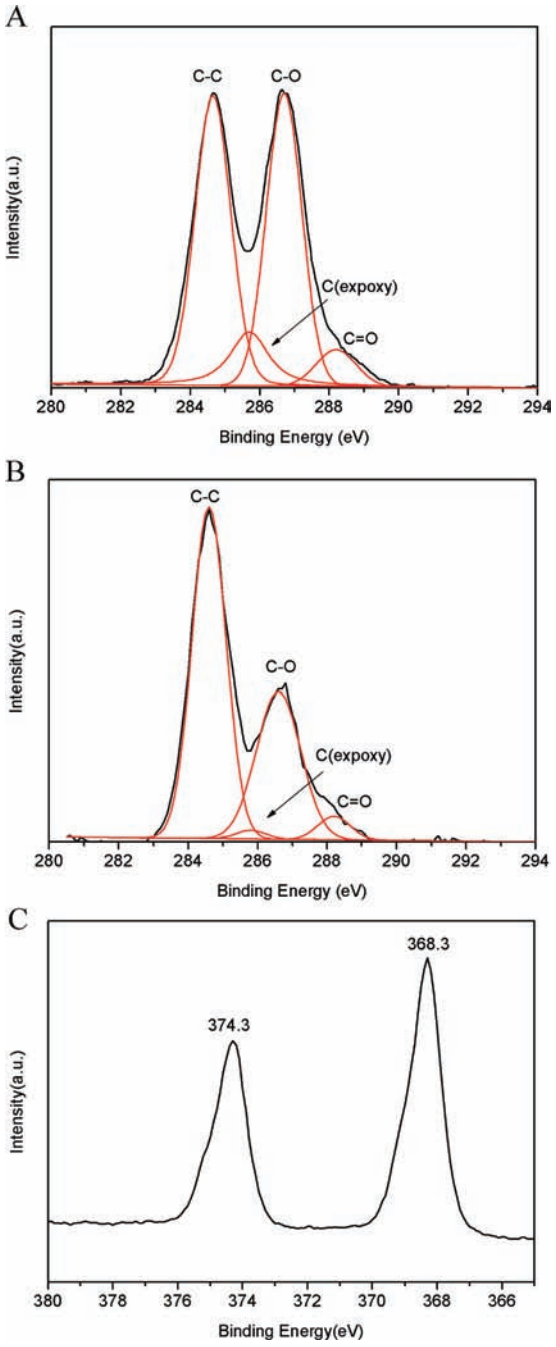

Figure 2. C 1s spectra of GO (A) and the products (B); the Ag 3d XPS spectrum of the products (C).

as shown in Figure 5B. These observations indicate that the increase of Ag^+ amounts is favorable for the formation of AgNPs with a larger size and higher density.

GO is covered with hydroxyl groups on the hexagonal basal plane[18] and thus can serve as a mild reducing agent. However, GO can only reduce Ag^+ under basic conditions.[8a] Indeed, it is reported that in the presence of plenteous NaOH, a Ag(OH) intermediate forms in the solution,[19,20] the reduction of which to Ag^0 followed by nucleation to form AgNPs is simultaneously accelerated by NaOH. On the other hand, GO can be converted into rGO rapidly under strong alkaline conditions.[21] Therefore, NaOH, the strong alkaline presented in our present system, plays a dual role: not only accelerating the reduction of

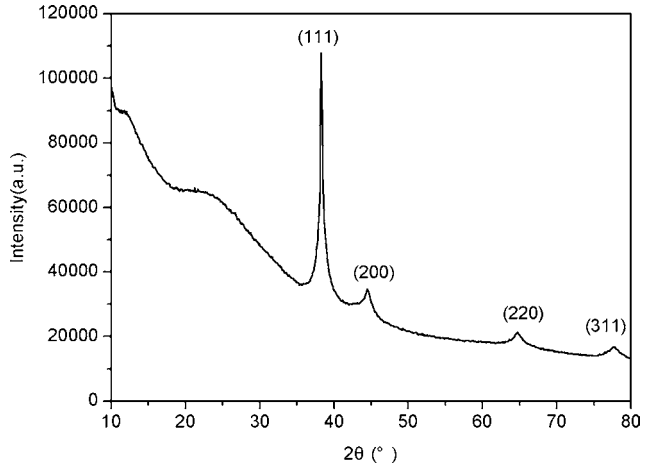

Figure 3. XRD pattern of products thus obtained.

Ag^+ by GO to form AgNPs but inducing the reduction of GO into rGO. As a result, AgNPs/rGO was formed finally.

We further explored the application of the composites for photocurrent generation in the visible range of light. Figure S1 shows the absorption spectrum of AgNPs/rGO modified ITO. This electrode exhibits an intense peak centered around 470 nm, indicating the strong ability of the electrode to absorb light in the visible spectrum range. The transient photocurrents of AgNPs, rGO, and AgNPs/rGO irradiated with visible light (λ > 400 nm) are shown in Figure 6. For AgNPs, a small anodic photocurrent of ca. 0.15 μA is obtained under visible light illumination (curve C), which can be attributed to the surface plasmon resonance excitation in the AgNPs, indicating the photogenerated electrons move to the bulk and finally transer to ITO and leave holes on the outer surface. For rGO, a small anodic photocurrent ca. 0.09 μA in intensity is observed under visible light illumination (curve B). In contrast, a prompt photocurrent is observed for AgNPs/rGO, the photocurrent intensity of which is about 1.46 μA. Compared with AgNPs and rGO, AgNPs/rGO exhibits a 32-fold and 16-fold enhancement of photocurrent intensity, respectively (curve A), suggesting the synergistic effect of both AgNPs and rGO in the composites. Thus, we come to the conclusion that rGO plays a positive role in the photocurrent generation of the modified electrode. On one hand, rGO can accept the electrons from the AgNPs; on the other hand, rGO can facilitate electron transfer within the composite film.[22]

We also examined the influence of the density of AgNPs on rGO sheets on the photocurrent generation properties of the AgNPs/rGO composites. The transient photocurrents of sample 2 and sample 3 irradiated with visible light (λ > 400 nm) are shown in Figure 7. Both the two samples exhibit anodic photocurrent, with 0.21 μA for sample 2 (curve B) and 0.53 μA for sample 3 (curve A) in intensity under visible light illumination. The relative intensity of the D to G bands was 0.92 and 0.95 for sample 2 and sample 3 (Figure S2, Supportig Information), respectively, demonstrating that the reduction degree of rGO remains similar in the three samples[23] while the density of particles on rGO sheets of sample 2, sample 1, and sample 3 increases with increased Ag^+ amounts. However, sample 1 shows the best generation of photocurrent, mainly due to the proper density of AgNPs decorated on rGO sheets. The particle density is too low for sample 2 and too high for sample 3, leading to unsatisfied intensity of the photocurrent

dx.doi.org/10.1021/ic300332x | Inorg. Chem. 2012, 51, 4742–4746

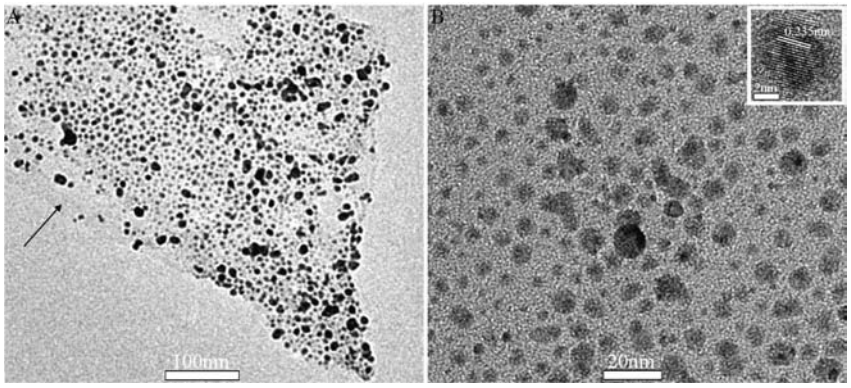

Figure 4. Low (A) and high (B) magnification TEM images of AgNPs/rGO. Inset: HRTEM image of a nanoparticle on the AgNPs/rGO.

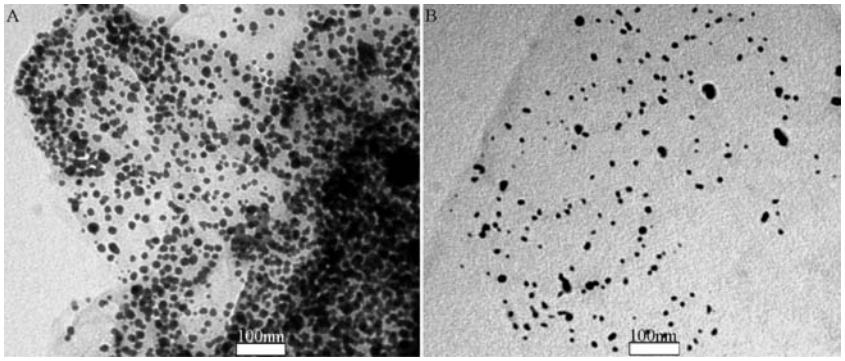

Figure 5. TEM images of the products of sample 2 (A) and sample 3 (B).

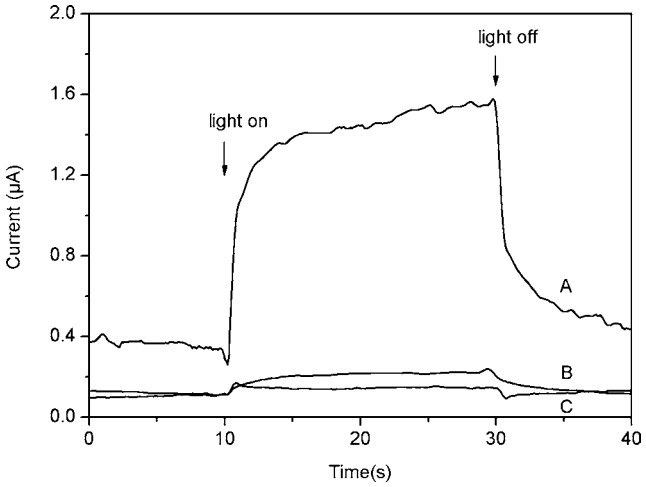

Figure 6. Photocurrent responses of AgNPs/rGO (A), rGO (B), and AgNPs (C) modified ITO electrode in a standard three-compartment cell along with a Pt wire counterelectrode and a reference electrode (Ag/AgCl) under white light illumination (λ >400 nm; input power, 100 mW/cm^2; electrolyte, 1 M Na_2SO_4 aqueous solution; electrode potential of 0 V vs Ag/AgCl).

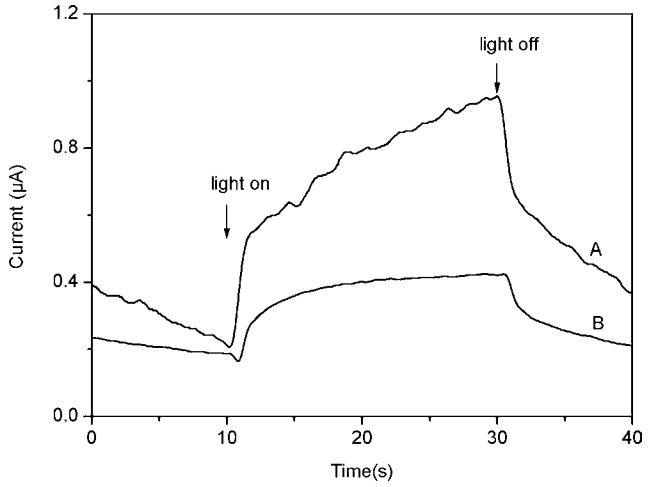

Figure 7. Photocurrent responses of sample 3 (A) and sample 2 (B) modified ITO electrode in a standard three-compartment cell along with a Pt wire counterelectrode and a reference electrode (Ag/AgCl) under white light illumination (λ >400 nm; input power, 100 mW/cm^2; electrolyte, 1 M Na_2SO_4 aqueous solution; electrode potential of 0 V vs Ag/AgCl).

owing to the inefficient electron−hole separation in the composites. On the basis of these observations, we conclude that the reduction degree of rGO is similar, and the density of particles decorated on rGO sheets plays a significant role in the photocurrent generation properties.

■ CONCLUSIONS

In summary, heating the mixture of graphene oxide (GO) and $AgNO_3$ aqueous solution in the presence of sodium hydroxide has been proven to be an effective strategy toward one-pot, rapid preparation of AgNPs/rGO without the involvement of other reducing agents and a surface modifier. The application of such a AgNPs/rGO in photocurrent generation has also been demonstrated. Compared to either pure AgNPs or rGO, the AgNPs/rGO composites show a great enhancement in photocurrent. Our present study is important because it provides us a practical, convenient, environmentally friendly

dx.doi.org/10.1021/ic300332x | Inorg. Chem. 2012, 51, 4742−4746

approach toward one-pot synthesis of AgNPs/rGO for applications.

■ ASSOCIATED CONTENT

Supporting Information

UV−vis absorption spectrum and Raman spectra. This material is available free of charge via the Internet at http://pubs.acs.org.

■ AUTHOR INFORMATION

Corresponding Author

*Phone/Fax: (+86)-431-85262065. E-mail: sunxp@ciac.jl.cn.

Notes

The authors declare no competing financial interest.

■ ACKNOWLEDGMENTS

This work was supported by the National Natural Science Foundation of China (No. 21175129) and the National Basic Research Program of China (No. 2011CB935800).

■ REFERENCES

(1) Guo, H.-L.; Wang, X.-F.; Qian, Q.-Y.; Wang, F.-B.; Xia, X.-H. *ACS Nano* **2009**, *3*, 2653.

(2) Kamat, P. V. *J. Phys. Chem. Lett.* **2011**, *2*, 242.

(3) Li, D.; Muller, M. B.; Gilje, S.; Kaner, R. B.; Wallace, G. G. *Nature Nanotechnol.* **2008**, *3*, 101.

(4) Liu, S.; Tian, J. Q.; Wang, L.; Li, H. L.; Zhang, Y. W.; Sun, X. P. *Macromolecules* **2010**, *43*, 10078.

(5) (a) Williams, G.; Kamat, P. V. *Langmuir* **2009**, *25*, 13869. (b) Williams, G.; Seger, B.; Kamat, P. V. *ACS Nano* **2008**, *2*, 1487. (c) Seger, B.; Kamat, P. V. *J. Phys. Chem. C* **2009**, *113*, 7990.

(6) Awazu, K.; Fujimaki, M.; Rockstuhl, C.; Tominaga, J.; Murakami, H.; Ohki, Y.; Yoshida, N.; Watanabe, T. *J. Am. Chem. Soc.* **2008**, *130*, 1676.

(7) (a) Wen, Y. Y.; Ding, H. M.; Shan, Y. K. *Nanoscale* **2011**, *3*, 4411. (b) Wu, T. S.; Liu, S.; Luo, Y. L.; Lu, W. B.; Wang, L.; Sun, X. P. *Nanoscale* **2011**, *3*, 2140.

(8) (a) Pasricha, R.; Gupta, S.; Srivastava, A. K. *Small* **2009**, *5*, 2253. (b) Lightcap, I. V.; Kosel, T. H.; Kamat, P. V. *Nano Lett.* **2010**, *10*, 577. (c) Liu, J. B.; Fu, S. H.; Yuan, B.; Li, Y. L.; Deng, Z. X. *J. Am. Chem. Soc.* **2010**, *132*, 7279. (d) Zhou, X.; Huang, X.; Qi, X.; Wu, S.; Xue, C.; Boey, F. Y.C.; Yan, Q.; Chen, P.; Zhang, H. *J. Phys. Chem. C* **2009**, *113*, 10843. (e) Li, J.; Liu, C. Y. *Eur. J. Inorg. Chem.* **2010**, *8*, 1244. (f) Xu, W. P.; Zhang, L. C.; Li, J. P.; Yang, L.; Li., H. H.; Ma, Y. N.; Wang, W. D.; Yu, S. H. *J. Mater. Chem.* **2011**, *21*, 4593. (g) Liu, S.; Tian, J. Q.; Wang, L.; Sun, X. P. *Carbon* **2011**, *49*, 3158. (h) Hassan, H. M. A.; Abdelsayed, V.; Khder, A. E. R. S.; AbouZeid, K. M.; Terner, J.; El-Shall, M. S.; Al-Resayes, S. I.; El-Azhary, A. A. *J. Mater. Chem.* **2009**, *19*, 3832. (i) Shen, J. F.; Shi, M.; Yna, B.; Ma, H. W.; Li, N.; Ye, M. X. *J. Mater. Chem.* **2011**, *21*, 7795. (j) Liu, S.; Tian, J. Q.; Wang, L.; Sun, X. P. *J. Nanopart. Res.* **2011**, *13*, 4539. (k) Zhang, Y. W.; Liu, S.; Wang, L.; Qin, X. Y.; Tian, J. Q.; Lu, W. B.; Chang, G. H.; Sun, X. P. *RSC Adv.* **2012**, *2*, 538. (l) Zhang, Z.; Xu, F. G.; Yang, W. S.; Guo, M. Y.; Wang, X. D.; Zhang, B. L.; Tang, J. L. *Chem. Commun.* **2011**, *47*, 6440. (m) Tang, X. Z.; Cao, Z. W.; Zhang, H. B.; Liu, J.; Yu, Z. Z. *Chem. Commun.* **2011**, *47*, 3084. (n) Shen, J.; Shi, M.; Li, N.; Yan, B.; Ma, H.; Hu, Y.; Ye, M. *Nano Res.* **2010**, *3*, 339.

(9) Hummers, W. S. Jr; Offeman, R. *J. Am. Chem. Soc.* **1958**, *80*, 1339.

(10) Gao, J.; Liu, F.; Ma, N.; Wang, Z.; Zhang, X. *Chem. Mater.* **2010**, *22*, 2213.

(11) Pimenta, M. A.; Dresselhaus, G.; Dresselhaus, M. S.; Cancado, L. G.; Jorio, A.; Saito, R. *Phys. Chem. Chem. Phys.* **2007**, *9*, 1276.

(12) (a) Dreyer, D. R.; Park, S. J.; Bielawski, C. W.; Ruoff, R. S. *Chem. Soc. Rev.* **2010**, *39*, 228. (b) Stankovich, S.; Dikin, D. A.; Piner, R. D.; Kohlhaas, K. A.; Kleinhammes, A.; Jia, Y.; Wu, Y.; Nguyen, S. T.; Ruoff, R. S. *Carbon* **2007**, *45*, 1558. (c) Guo, Y.; Guo, S.; Ren, J.; Zhai, Y.; Dong, S.; Wang, E. *ACS Nano* **2010**, *4*, 4001.

(13) Park., S.; An, J.; Piner, R. D.; Jung, I.; Yang, D.; Velamakanni, A.; Nguyen, S. T.; Ruoff, R. S. *Chem. Mater.* **2008**, *20*, 6592.

(14) Pol, V. G.; Srivastava, D. N.; Palchik, O.; Palchik, V.; Slifkin, M. A.; Weiss, A. M.; Gedanken, A. *Langmuir* **2002**, *18*, 3352.

(15) Sun, X.; Dong, S.; Wang, E. *Macromolecules* **2004**, *37*, 7105.

(16) (a) Yang, Y.; Ren, L.; Zhang, C.; Huang, S.; Liu, T. *ACS Appl. Mater. Interfaces* **2011**, *3*, 2779. (b) Falcao, E. H. L.; Blair, R. G.; Mack, J. J.; Viculis, L. M.; Kwon, C. W.; Bendikov, M.; Kaner, R. B.; Dunn, B. S.; Wudl, F. *Carbon* **2007**, *45*, 1367. (c) Cong, H. P.; He, J. J.; Lu, Y.; Yu, S. H. *Small* **2010**, *6*, 169. (d) Chandra, V.; Park, J.; Chun, Young.; Lee, J. W.; Hwang, I.; Kim, K. S. *ACS Nano* **2010**, *4*, 3979.

(17) Yang, J.; Dennis, R.; Sardar, D. *Mater. Res. Bull.* **2011**, *46*, 1080.

(18) Kannan, P. R.; Swami, A.; Srisathiyanarayanan, D.; Shirude, P. S.; Pasricha, R.; Mandale, A. B.; Sastry, M. *Langmuir* **2004**, *20*, 7825.

(19) Wang, X.; Wu, H.; Kuang, Q.; Huang, R.; Xie, Z.; Zheng, L. *Langmuir* **2010**, *26*, 2774.

(20) Nishimure, S.; Mott, D.; Takagaki, A.; Maenosono, S.; Ebitani, K. *Phys. Chem. Chem. Phys.* **2011**, *13*, 9335.

(21) Fan, X.; Peng, W.; Li, Y.; Li, X.; Wang, S.; Zhang, G.; Zhang, F. *Adv. Mater.* **2008**, *20*, 4490.

(22) Hayashi, H. I.; Lightcap, V.; Tsujimoto, M.; Takano, M.; Umeyama, T.; Kamat, P. V.; Imahori, H. *J. Am. Chem. Soc.* **2011**, *133*, 7684.

(23) Kudin, K. N.; Ozbas, B.; Schniepp, H. C.; Prud'homme, R. K.; Aksay, I. A.; Car, R. *Nano Lett.* **2008**, *8*, 36.